

## Surface-engineered double-layered fabrics for continuous, passive fluid transport

*Mohammad Soltani<sup>1</sup>, Sudip Kumar Lahiri<sup>1</sup>, Sadaf Shabanian<sup>2</sup>, Kevin Golovin<sup>1</sup>*

<sup>1</sup> Department of Mechanical and Industrial Engineering, University of Toronto, Toronto, Ontario, M5S 3G8, Canada

<sup>2</sup> School of Engineering, University of British Columbia, Kelowna, British Columbia, V1V 1V7, Canada.

E-mail: kevin.golovin@utoronto.ca

**Video S1:** Transport of an 8  $\mu$ L water droplet deposited at a distance from the stitches of the double-layer design.

**Video S2:** The water droplet transport to the patterned channel through the stitches.

Table S1. Advancing/Receding contact angle of water and artificial sweat on exposed and unexposed areas of the fabric versus plasma time. The contact angles were measured using the sessile drop method.

Plasma Time (s)	Water				Artificial sweat			
	Exposed		Back		Exposed		Back	
	$\theta_{adv}$ [°]	$\theta_{rec}$ [°]	$\theta_{adv}$ [°]	$\theta_{rec}$ [°]	$\theta_{adv}$ [°]	$\theta_{rec}$ [°]	$\theta_{adv}$ [°]	$\theta_{rec}$ [°]
0	151±2	144±2	156±2	149±2	149±2	144±1	151±1	149±2
10	146±4	129±5	152±2	145±2	144±2	124±4	149±2	147±1
20	146±5	119±5	152±2	140±2	142±3	111±4	147±1	142±2
30	141±5	91±6	150±2	142±2	141±4	99±5	146±2	139±2
40	140±4	88±6	147±2	138±2	137±3	79±7	142±1	139±2
50	137±4	76±7	148±2	135±2	126±2	0	142±2	136±2
60	118±9	0	149±2	133±3	114±6	0	140±2	136±2
70	97±14	0	146±1	138±2	93±10	0	140±2	133±3
80	94±12	0	150±2	139±3	86±7	0	141±3	132±2
100	56±12	0	149±2	140±3	55±9	0	139±2	134±3
120	29±7	0	147±3	140±3	24±5	0	136±2	132±3
140	0	0	151±3	142±3	0	0	139±3	130±3
160	0	0	149±3	144±3	0	0	134±4	129±4



Figure S1: Time-lapsed images of water droplet wetting the silica particle-patterned channels on the PDMS-coated superhydrophobic fabric.

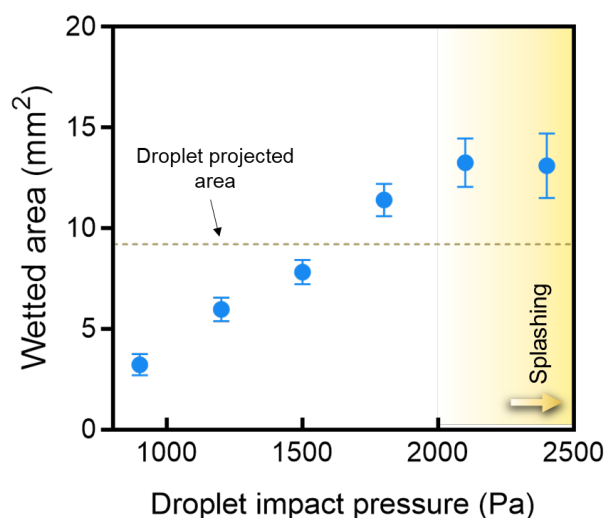


Figure S2: The dynamic intrusion test for pressures exceeding the breakthrough pressure. The wetted area underneath the water droplet (21  $\mu\text{L}$ ) increases by increasing the impact height (The yellow region indicates the onset of splash).

Table S2. Physical properties of three different type of fabrics.

Fabric	Type I	Type II	Type III
<b>Thickness (<math>\mu\text{m}</math>)</b>	590 $\pm$ 20	380 $\pm$ 10	610 $\pm$ 10
<b>Composition</b>	Polyester	Nylon	Nylon
<b>Weight (<math>\text{g}/\text{m}^2</math>)</b>	180	165	195

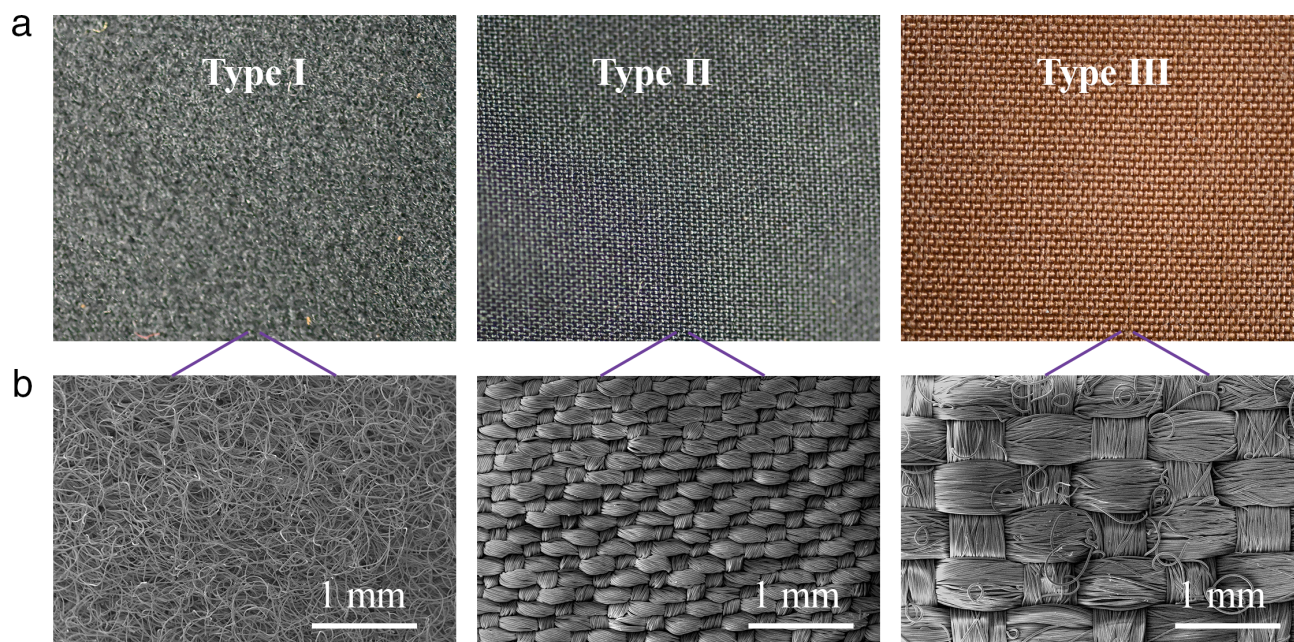


Figure S3. a) Optical images of the three different types of fabrics examined in this work. Type I was primarily used in this study. The two other fabrics were used to compare their wettability behavior and breakthrough pressure after selective plasma treatment. b) SEM images of the three different fabric types.

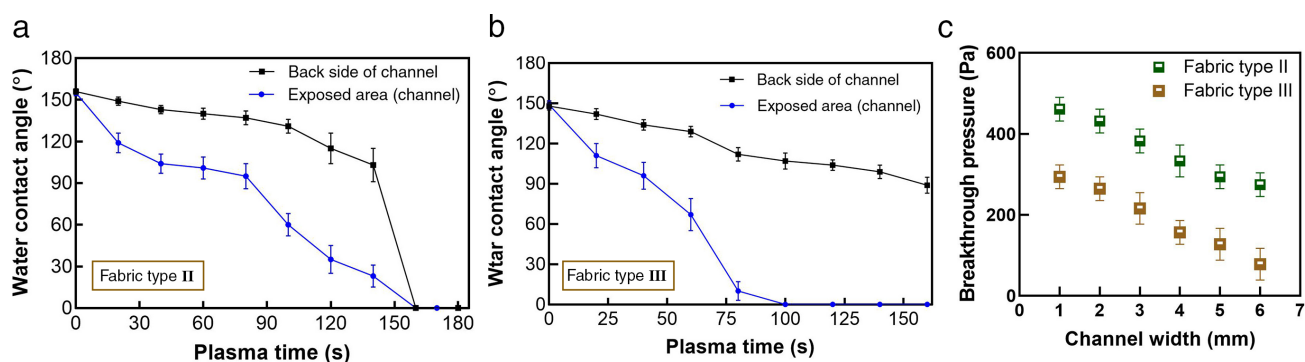


Figure S4. Water contact angles of the channel and its back side for different plasma treatment time. a) Fabric type II, b) Fabric type III. c) The static breakthrough pressure of type II and III fabrics, patterned with channels of 1 – 6 mm width, using 140 s of plasma treatment.



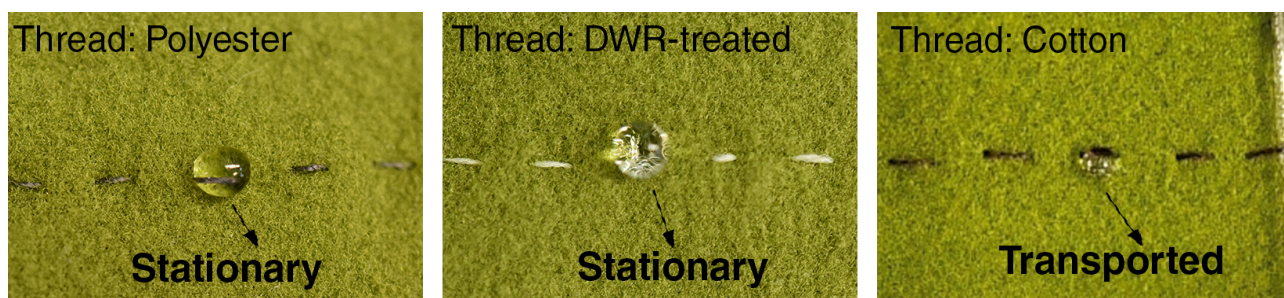


Figure S5: The liquid transport performance of different thread materials. 5 seconds after depositing the droplet, the 9  $\mu$ L water droplet was transported only through the cotton thread, whereas it remained stable on the less wettable polyester and DWR-treated thread surfaces.

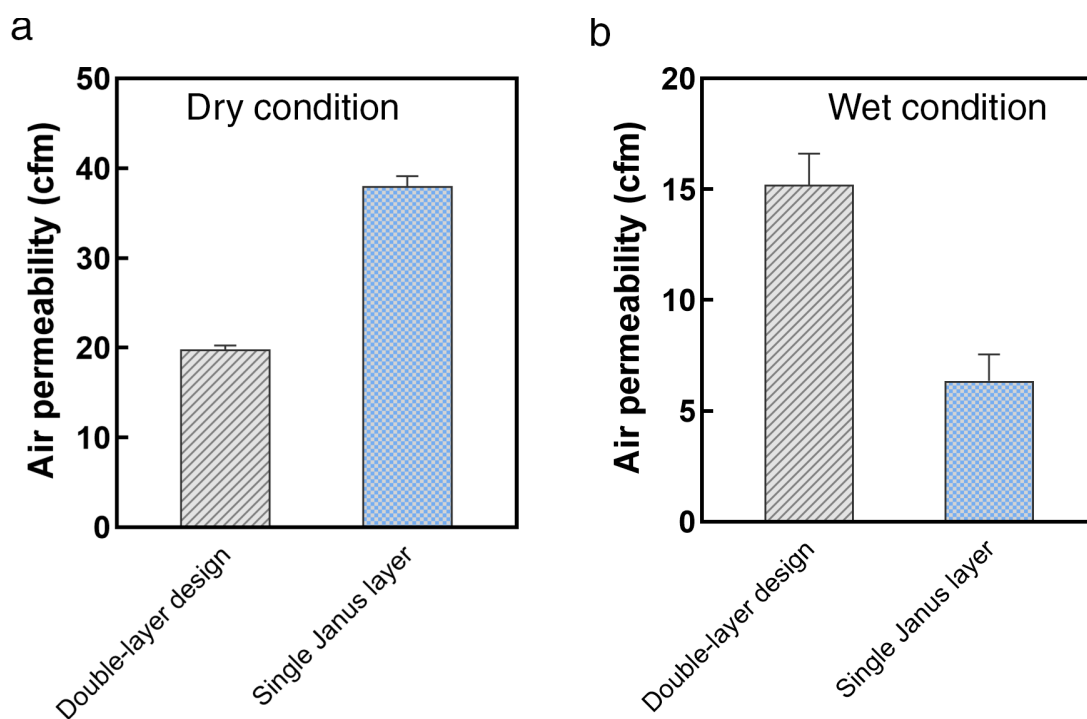


Figure S6: The air permeability of the double-layered design and single Janus layer in a) dry condition and b) wet condition, both containing the same amount of water.

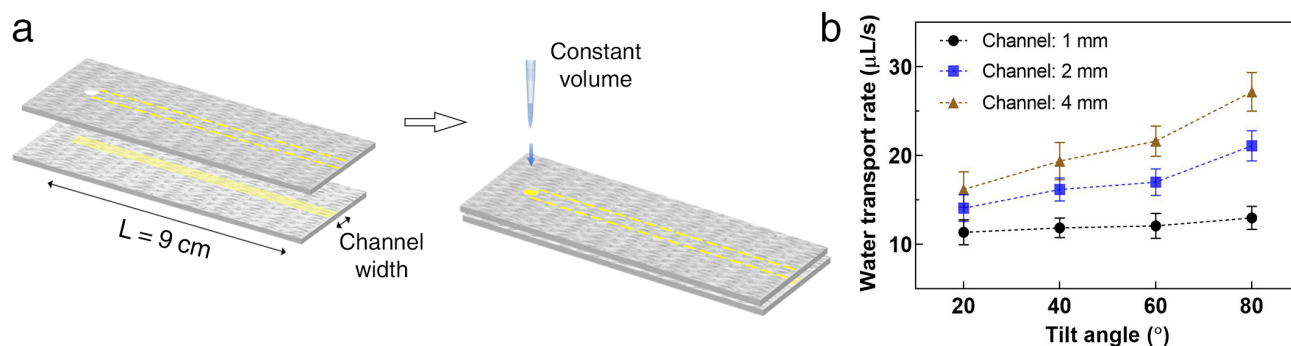


Figure S7. a) Schematic of the experiment conducted to measure the liquid transport rate along the wettability channels without stitches. The surfaces were tested at different tilt angles with respect to the channel direction, and a constant droplet volume was supplied to a perforated hole on the top layer. b) The water transport rate measured at different tilt angles for channels of 1, 2, and 4 mm width.

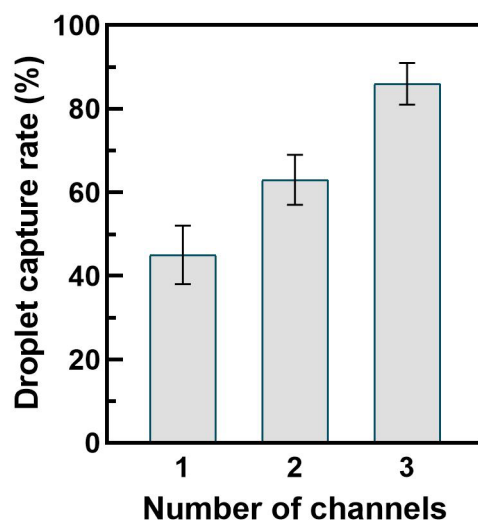


Figure S8. The water droplet capture rate for the different number of channels intersecting the moving droplets. For the artificial sweating test, the channels can be engineered to maximize droplet capture as they slide down the substrate.

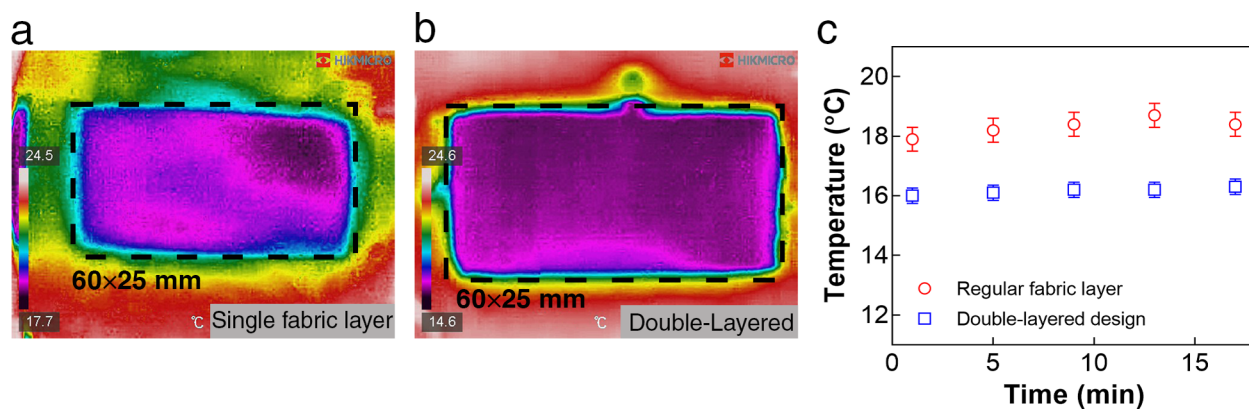


Figure S9. The temperature map of a) a single fabric layer covered with an insulating layer and b) the fabric assembly discussed in Figure 6b (obtain from infrared images). c) The temperature of the exposed parts of the single fabric layer covered with the insulation layer, and the reservoir of the double-layered design.